Curvature effects on wave propagation in an infinite pipe

M. Ratassepp, A. Klauson

Tallinn University of Technology, Department of Mechanics, 5 Ehitajate tee, Tallinn 19086, Estonia,
e-mail : madisr@hot.ee

Abstract

Advanced research into non-destructive control of industrial pipeworks provides several acoustical methods for inspection of their structural integrity. Applying guided waves is one possible solution to detect and identify different flaws. Many studies have shown the importance of complex waves describing the interaction phenomena at the vicinity of the defects, modeled as geometrical discontinuities. Therefore it is important to understand the behavior of this type of waves in order to describe correctly wave interaction with the discontinuities like joints, cracks and solid deposits. This paper presents theoretical study of axi-symmetric longitudinal guided and complex wave propagation and in elastic pipes. The asymptotic dispersion equation of the pipe gives a comprehensive representation of all wave types presented in the structure: propagating, non-propagating and inhomogeneous waves. Dispersion curves corresponding to real, imaginary wave number for the longitudinal modes in a wide frequency-thickness range and different radii of the pipe are given.

Keywords: non-destructive evaluation, cracks, semi-infinite pipe, guided waves, inhomogeneous waves.

Introduction

In several industries the inspection of pipelines is an important problem and the need for reliable assessment applications has been announced by numerous pipeline accident reports [1]. Attractive solution for this is to apply ultrasonic guided waves in the pipe inspection because this method allows to investigate inaccessible areas (insulated pipes) and long distances of the pipe wall from a single point. Therefore this unique technique widely reduces inspection time and costs compared to the ordinary point-by-point testing in large pipeworks. The practical study in this field has been very intensive and lead to implementation of various testing techniques and creation of commercial transducer systems [2-10].

Defects such as cracks and corrosion pits that can develop in circumferential direction in the pipe can be detected by screening the pipeline with axially propagating guided waves. As the guided waves travel through the pipe wall, they are affected by the features they encounter and are scattered. The scattering of guided elastic waves from defects located within a waveguide has been one of the major research targets in nondestructive evaluation [11-19] but still the understanding of all the details of this phenomenon is not quite clear. The defect serves as a source of new guided waves, which are dependants of the parameters of the defect, besides different non-propagating and complex waves occur in the waveguide interfering the near field measurements. Therefore the explanation of the nature of different wave modes would be a very useful tool in the evaluation of specific defect types in waveguide structures.

In cases when tester device is placed near the edge of the waveguide or it is demanded to detect through-thickness cracks it is beneficial to study near edge field of the waveguide structure. The wave field near the edge is accompanied by evanescent waves that do not propagate into the pipe and can perturb signal interpretation in near edge measurements [19]. A considerable amount of work has been done on the reflection of guided waves at a free edge of plates and rods [20-25] but to the author's knowledge the guided wave scattering problem in cylindrical pipes [13,26] has received much less attention. It is probably so due to the fact that the axisymmetric wave propagation in large radius thin-walled pipe structure resembles to Lamb waves in a plate as was shown by Silk and Bainton [27]. However, the effect of curvature becomes essential in wave propagation characteristics in thick pipes at low frequencies and therefore needs some further study.

The aim of present study is to develop analytical wave propagation model for cylindrical pipes to help interpreting the behavior of longitudinal wave modes $L(0,1)$, $L(0,2)$, … The properties of different wave modes (propagating, non-propagating, inhomogeneous) are expressed in the form of frequency dependent dispersion curves, presenting phase velocities and wave numbers and through-thickness mode shapes. This paper focuses primarily on the study of curvature effects of longitudinal wave propagation characteristics.

Theory. Modes of elastic wave propagation in hollow cylinder

The general three-dimensional solution of the wave propagation in hollow cylinder of infinite extent (Fig.1) was documented by Gazis [28] already in 1959. In the framework of linear theory of elasticity he obtained a characteristic equations, which described three special families of modes identified as symmetric longitudinal and torsional modes and nonaxisymmetric flexural modes. Later Meitzler [29] used conventional labeling for these modes as $L(0,m)$, $T(0,m)$ and $F(n,m)$, where first index indicates the circumferential order and second number is a counter in order of appearance of different modes in one wave family. In general, there are an infinite number of individual modes within each wave family, whose wave numbers ξ, for a given frequency-pipe thickness product fd, represent permissible solutions to a characteristic dispersion equation (a brief derivation of the dispersion equation, displacements and stresses is provided in Appendix A)

$$Det\left|G(c_L, c_T, a, b, f)\right| = 0, \qquad (1)$$

where c_L, c_T – longitudinal and shear velocity of the medium a, b – inner and outer radius of the pipe, respectively. In general, the roots of the dispersion equation can be real, imaginary or complex. A purely real solution describes a wave mode propagating with no attenuation; imaginary solution describes a nonpropagating, or evanescent mode. This is essentially a mode that is critically damped and thus does not propagate. Mostly, the interest in using these non-propagating modes for describing stress and displacement fields very close to the wave sources (for example discontinuities), but it is unimportant in the far field. Complex roots describe a propagating wave mode that is attenuating with distance from the source and are called inhomogeneous wave modes. Although several investigation have been performed on the explanation of complex roots in plates and rods [20, 21], the nature of complex frequency spectrum of the pipe is not thoroughly investigated. One reason for this is that the wave propagation in large radius pipe structure is very similar to the wave propagation in a plate and thus using complicated pipe solutions was not reasoned. However, many inspection procedures have been adjusted to low frequencies where the effect of the curvature of the pipe might become noticeable in wave propagation and intensifies when the pipe inner radius $a \rightarrow 0$, resulting the wave modes of a solid cylinder.
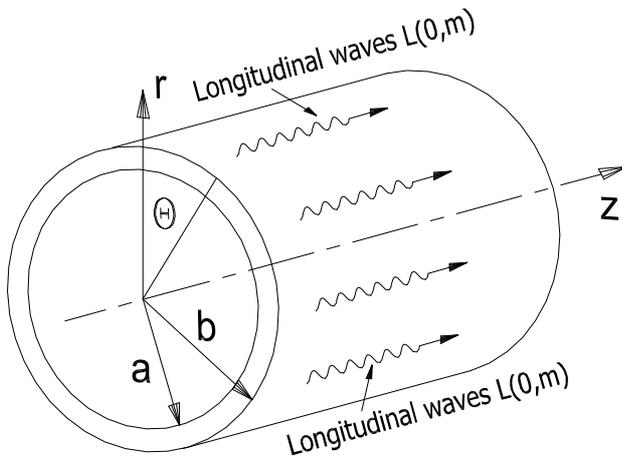
Fig. 1. **Formulation of the problem in cylindrical coordinates**

Numerical results. Dispersion curves and mode shapes

The dispersion curves are very important to the post processing of the inspection results, from which the, defects and other features of the structure can be identified, located and sized. A sample phase and group velocity dispersion curves are presented in Fig.2 and Fig.3, correspondingly. Material properties employed in this study are shown in Table I. There are many different longitudinal wave modes $L(0,m)$ which can propagate at different speeds, and they are, in general, frequency-dependent, or dispersive. Group velocity curves in Fig.3 indicate the speed of propagation of wave packet and are

therefore the curves of particular interest for long-range propagation. The effect of dispersion on a propagating mode means that the shape of the wave packet is distorted and the peak amplitude of the packet decreases. Thus, this phenomenon refers to reduction in resolution and therefore is undesirable in long range testing. To avoid dispersion effects when using tone bursts of limited bandwidth the excitation points must be chosen in regions where the rate of group velocity change with respect to frequency is minimal. Operating points of this type are marked by circles on the group velocity dispersion curves in Fig.3.

Table I. **Material parameters used for of the pipe.**

ρ (kg/m^3)	c_L (m/s)	c_T (m/s)	E (MPa)	υ
7800	5840	3150	200	0.3

Next parameter of interest that affects the wave propagation is the curvature. From the figures it can be clearly seen that the effect of the curvature of the pipe is most noticeable at low frequencies. As the frequency increases the pipe starts to vibrate like a plate. The effect of changing the inner radius from $a = 16.5$ to $a = 0$ is demonstrated by transitions "I" and "II". This will cause shift of operating points into higher frequencies and the small change of group velocities as it is seen from transitions $1 \rightarrow 2$ and $3 \rightarrow 4$ in Fig. 3. It was also found that the difference of the group velocity speed of the operating point of $L(0,2)$ mode is approximately 4% between in a plate and a pipe with thickness to inner radius ratio $d/a = 0.5$. Therefore in long-range inspection procedures the curvature effect is rather perceivable.

In addition to real wave modes, there also exists at any given frequency a finite number of imaginary and an infinite number of complex wave modes. In order to obtain all the roots of interest a simple root finding routine was used. This was based on finding the local minima of the absolute value of the dispersion equation (A.4). When calculating complex roots, Hankel functions were used instead of Bessel functions through (A.5-A.6) because they provided better numerical stability. When Hankel functions $H_n^{(1)}(x) \rightarrow 0$, $H_n^{(2)}(x) \rightarrow 0$ and $x \gg 1$ the asymptotic expressions were used

$$H_n^{(1)}(x) = \sqrt{\frac{2}{\pi x}} e^{i(x - n\pi/2 - \pi/4)},$$

$$H_n^{(2)}(x) = \sqrt{\frac{2}{\pi x}} e^{-i(x - n\pi/2 - \pi/4)}. \qquad (2)$$

A number of wave modes have been represented in Fig. 4 in a large frequency-thickness range $fd = [0 \ldots 10]$ MHz-mm. The complex roots are extensions of the higher-order wave branches below their cutoff frequencies and are denoted as C_1, C_2, . . . The complex branches disappear at those frequencies where new real or purely imaginary branches appear. Thus, with an increase in frequency, a nonpropagating mode can decay more slowly and eventually become a propagating mode, but at some frequencies the opposite is also true. As a matter of fact the complex roots occur in fours, one in each of the four quadrants of the ζ plane, while the real and imaginary solutions occur in pairs. Therefore the selection of proper
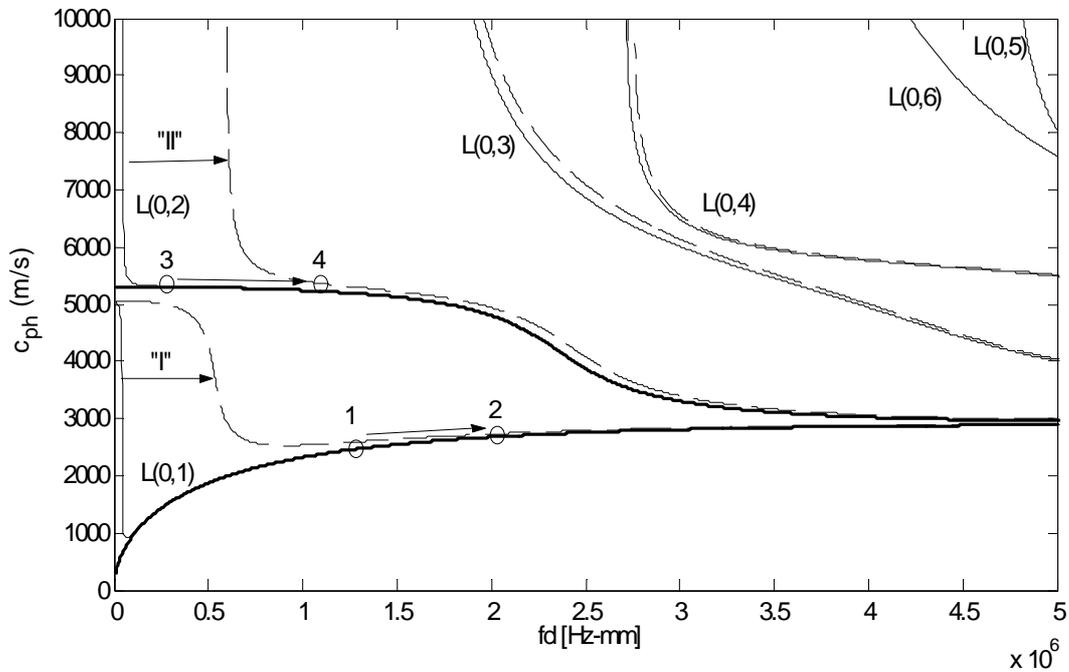
Fig. 2. **Phase velocity dispersion curves for (——) plate, (——) pipe with a =16.5 mm, b = 17.5 mm, (— —) solid cylinder b = 17.5 mm.**
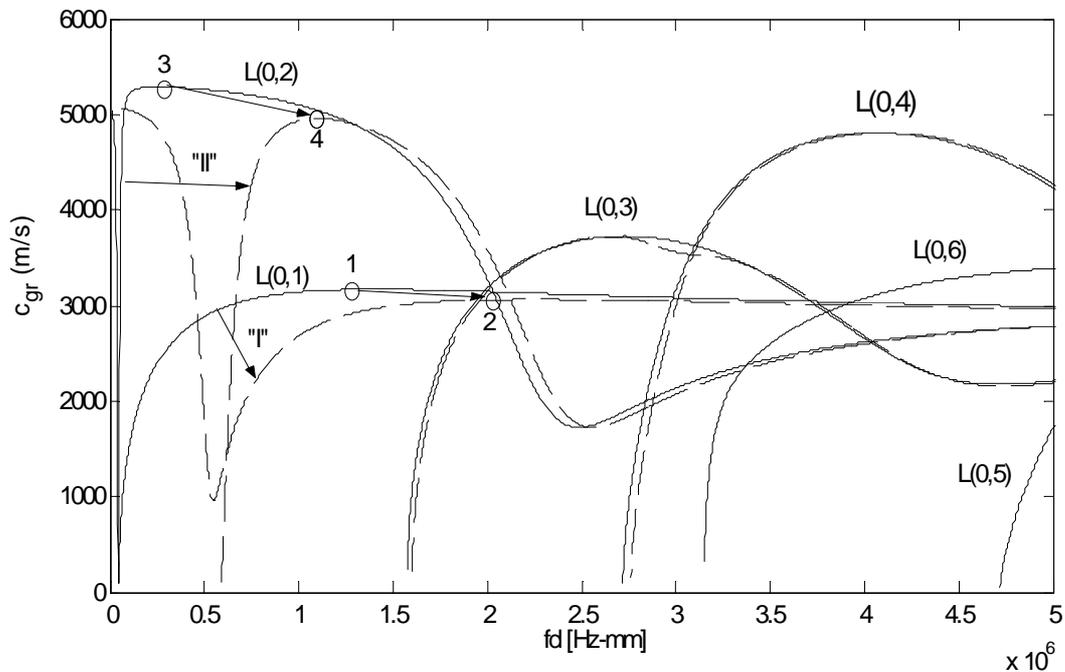
Fig. 3. **Group velocity dispersion curves for (——) pipe with a =16.5 mm, b = 17.5 mm, (— —) solid cylinder b = 17.5 mm.**

root must be used in solution [21] to fulfill the physical meaning of the scattering mechanism near discontinuity, the nonpropagating and inhomogeneous modes must decay with the distance from the source. Fig. 5 shows the evolution of lower order complex and imaginary modes when changing the inner and outer radius of the pipe. New complex mode C_0 appears which is the extension of $L(0,2)$ mode below its cutoff frequency. Remarkable change is seen in behavior of dispersion curves when pipe becomes a solid cylinder, however the curvature effect is decreasing when $Im(\xi)$ is increasing.

Another important characteristics that describe wave modes are their displacement and stress fields. Each mode has a unique through-thickness mode shapes, which assist us selecting right wave mode for a particular testing operation. Axisymmetric longitudinal wave modes have two displacement (A.7) and three stress components (A.8), each of them varying across the thickness of the pipe wall
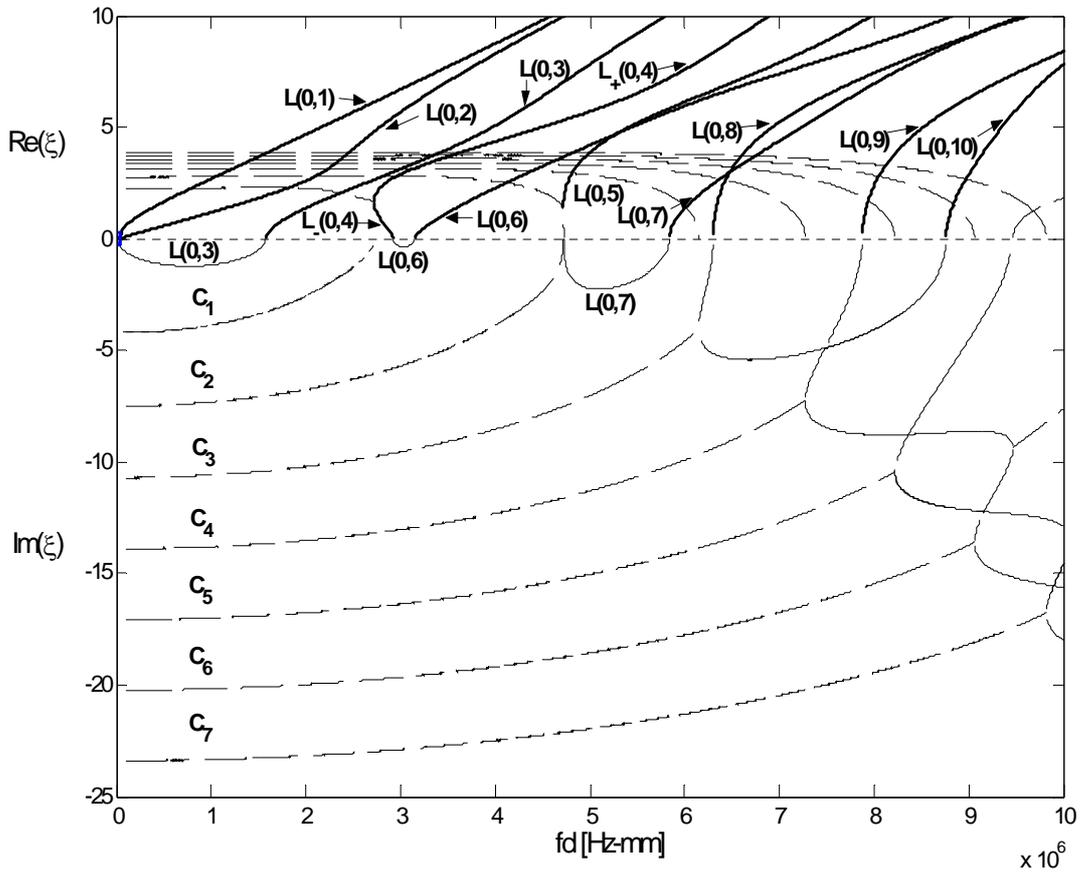
Fig. 4. **Axial wavenumber ξ dispersion curves. (——) real and imaginary modes, (— —) complex modes for a pipe. a = 17.5 mm, d = 1 mm**.
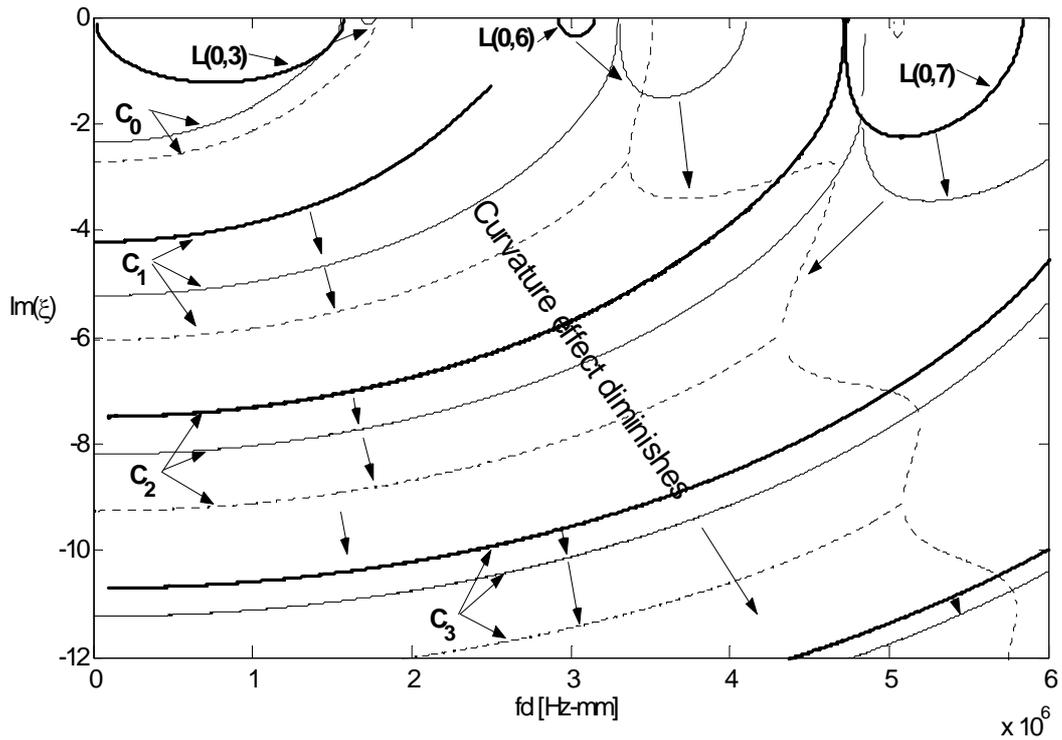
Fig. 5. **Im(ξ) dispersion curves. (——) a = 17.5 mm, d = 1 mm, (——) a = 2 mm, d = 17.5 mm, (— — —) a = 0, d = 17.5 mm**.

and in frequency space. In addition the variation of the thickness of the pipe can change the mode shapes. These effects are shown in Fig.6-8 for different wave modes at different frequencies. It can be seen that the symmetry and antisymmetry of displacement profiles (cases a) in Fig. 6 and Fig.7, which is inherent for plate structures, is corrupted in thick pipes (cases b). Moreover, the changes can be rather profound. For instance, at low frequencies

the mode $L(0,1)$ becomes a compressional wave as it is seen in Fig. 6 at frequency $fd = 0.1$ MHz-mm. The wave field of higher order complex modes (see C_6 in Fig.8) changes rapidly across the thickness of the pipe and therefore their amplitudes in scattering process must be smaller than propagating waves when the scattered has a flat boundary (plate).
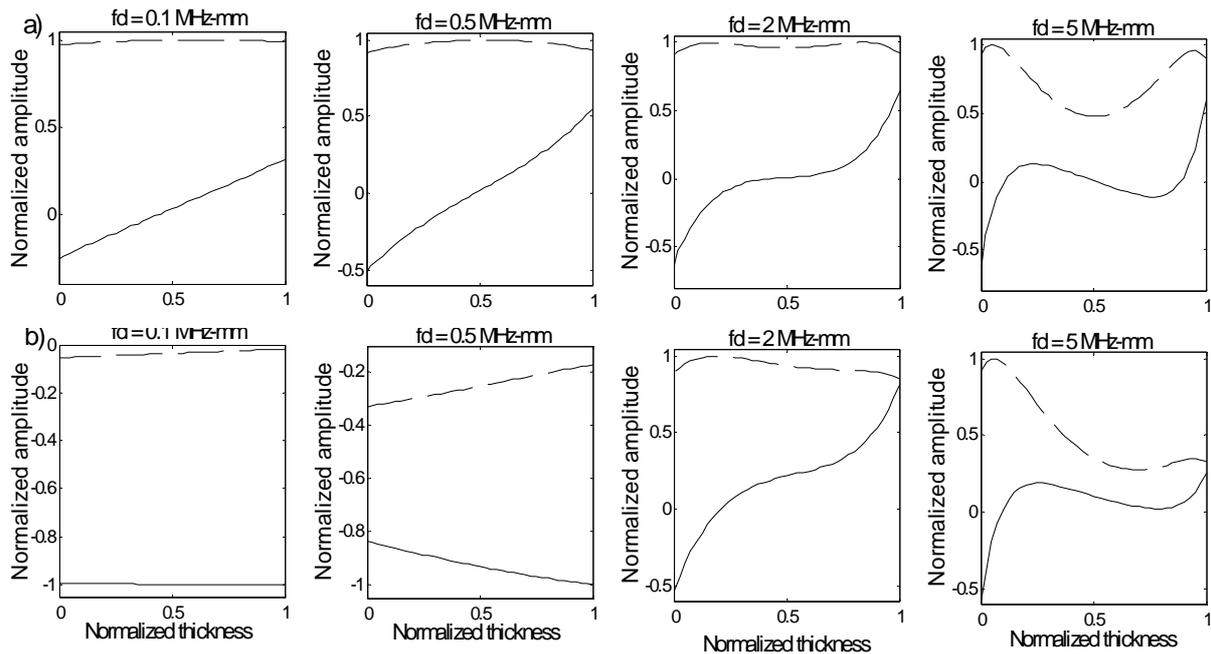
Fig. 6. **Axial u_z ($\longrightarrow$) and radial u_r ($--\rightarrow$) displacements for $L(0, 1)$ mode. a) a =17.5 mm, d = 1 mm; b) a = 8.75 mm, d = 17.5 mm**
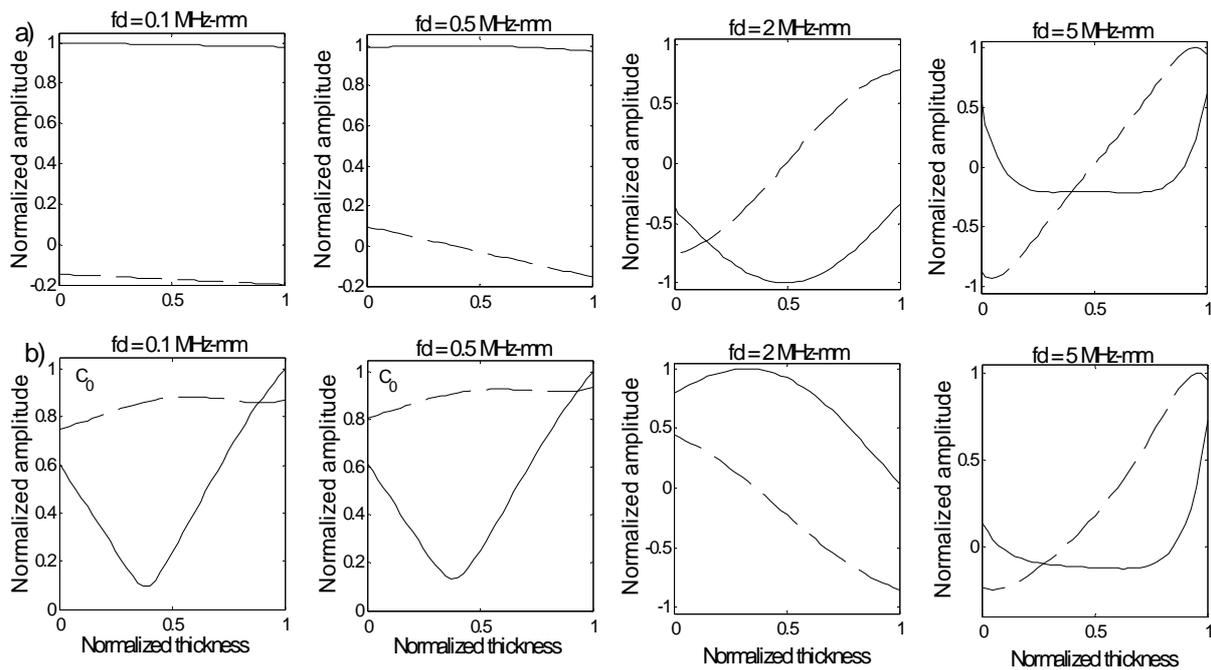
Fig. 7. **Axial u_z ($\longrightarrow$) and radial u_r ($--$) displacements for $L(0, 2)$ and C_0 mode: a) a =17.5 mm, d = 1 mm; b) a = 8.75 mm, d = 17.5 mm.**
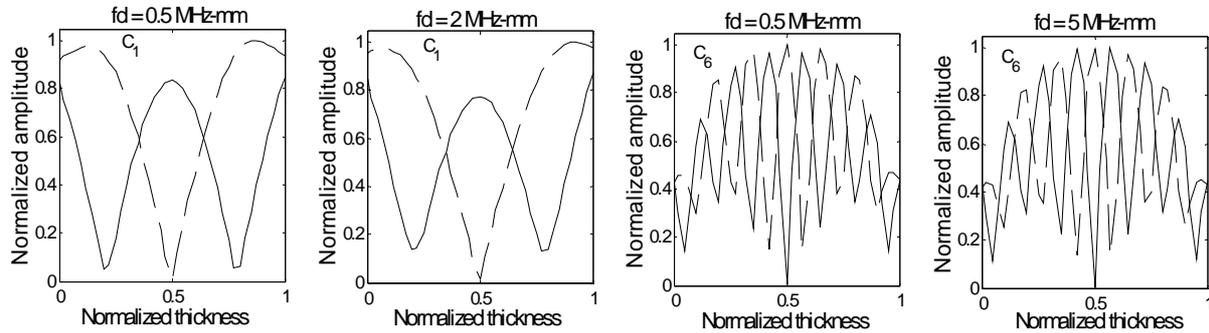
Fig. 8. **Module of axial u_z (——) and radial u_r (— —) displacements for C_1 and C_6 mode: a =17.5 mm, d = 1 mm**.

Conclusions

A compact analytical theory of axisymmetric longitudinal wave propagation in infinite pipe was given. The dispersion curves of propagating, nonpropagating and inhomogeneous wave modes were presented for various thickness-inner radius ratios. From the analysis of group velocity frequency spectrum and through-thickness mode shapes at different frequencies the fact that curvature affects the wave propagation at lower frequencies was validated.

Acknowledgements

References

1. **National Transportation Safety Board**. Natural gas pipeline rupture and fire Near Carlsbad, New Mexico. August 19. 2000. www.viadata.com/f_library.htm.

2. **Cawley P., Lowe M. J. S., Alleyne D. N.et al.** Practical long range guided wave testing: applications to pipes and rail. Materials Evaluation. 2003. Vol. 61. P.66–74.

3. **Barshinger J., Rose J. L., Avioli M. J.** Guided wave resonance tuning for pipe inspection. Journal of Pressure Vessel Technology. 2002. Vol. 124. P.303–310.

4. **Li J., Rose J. L.** Excitation and propagation of non-axisymmetric guided waves in a hollow cylinder. Journal of the Acoustical Society of America. 2001. Vol. 109. Issue 2. P.457-464.

5. **Tua P. S.** et al. Detection of cracks in cylindrical pipes and plates using piezo-actuated Lamb waves. Meas. Sci. Technol. 2005. Vol. 14. P. 1242-1352.

6. **Mijarez R., Gaydecki P, Burdekin M**. An axisymmetric guided wave encoded system for flood detection of oil rig cross-beams. Meas. Sci. Technol. 2005. Vol. 16. P. 2265–2274.

7. **Hay T. R., Rose J. L.** Fouling detection in food industry using ultrasonic guided waves. Food Control. 2002. Vol. 14. P. 481-488.

8. **Tucker R. W., Kercel S. W., Varma V. K.** Characterization of gas pipeline flaws using wavelet analysis. QCAV (Quality Control Using Artificial Intelligence), Gatlinburg, TN. May 2003.

9. **Zhao X.** et al. In-line nondestructive inspection of mechanical dents on pipelines with guided shear horizontal wave electromagnetic acoustic transducers. J. of Pressure Vessel Technology. 2005. Vol. 127, Issue 3. P. 304-309.

10. **Kwun H., Kim S. Y.** and **Light G. M.** Long-range guided wave inspection of structures using the magnetostrictive sensor. J. Korean Soc. for Nondestructive Testing. 2001. Vol. 21. P. 383-390.

11. **Rokhlin S..** Diffraction of Lamb waves by a finite crack in an elastic layer. Journal of the Acoustical Society of America. 1980. Vol. 67, Issue 4. P. 1157-1165.

12. **Rokhlin S.** Resonance phenomena of Lamb waves scattering by a finite crack in a solid layer. Journal of the Acoustical Society of America. 1981. Vol. 69, Issue 4. P. 922-928.

13. **Ditri J. J.** Utilization of guided elastic waves for the characterization of circumferential cracks in hollow cylinder. Journal of the Acoustical Society of America. 1994. Vol. 96, Issue 6. P. 3769-3775.

14. **Valle C., Niethammer M., Qu J., Jacobs L. J.** Crack characterization using guided circumferential waves. Journal of the Acoustical Society of America. 2001. Vol. 110, Issue 3. P. 1282-1290.

15. **Lowe M. J. S., Diligent O.** Low-frequency reflection characteristics of the S_0 Lamb wave from a rectangular notch in a plate. Journal of the Acoustical Society of America. 2002. Vol. 111. Issue 1. P. 64-74.

16. **Lowe M. J. S., Cawley P.** et al. The low-frequency reflection characteristics of the fundamental antisymmetric Lamb wave A_0 from a rectangular notch in a plate. Journal of the Acoustical Society of America. 2002. Vol. 112. Issue 6. P. 2612-2622.

17. **Castaigs M., Clezio E. Le, Hosten B.** Modal decomposition method for modeling the interaction of Lamb waves with cracks. Journal of the Acoustical Society of America. 2002. Vol. 112. Issue 6. P. 2567-2582.

18. **Benz R., Niethammer M., Hurlebaus S., Jacobs L. J.** Localization of notches with Lamb waves. Journal of the Acoustical Society of America. 2003. Vol. 114, Issue 2. P. 677-685.

19. **Diligent O.** Interaction between fundamental Lamb modes and defects in plates.PhD thesis Imperial College London. 2003.

20. **Torvik P. J..** Reflection of wave trains in semi-infinite plates. Journal of the Acoustical Society of America**. 1977. Vol. 41. Issue 2. P. 346-353.

21. **Zemanek J.** An Experimental and theoretical investigation of elastic wave propagation in a cylinder. Journal of the Acoustical Society of America. 1972. Vol. 51. Issue 1. P. 265-282.

22. **Cho Y., Rose J. L.** A boundary element solution for a mode conversion study on the edge reflection of Lamb waves. Journal of the Acoustical Society of America**. 1996**. Vol. 99. Issue 4. P. 2097-2109.

23. **Galan J. M., Abascal R.** Lamb mode conversion at edges. A hybrid boundary element-finite-element solution. Journal of the Acoustical Society of America. 2005. Vol. 117. Issue 4. P. 1777-1784.

24. **Gregory R. D., Gladwell I.** The reflection of a symmetric Rayleigh-Lamb wave at the fixed of free edge of plate. J. of Elasticity.1983. Vol. 13. P. 185-206.

25. **Morvan B., Wilkie-Chancellier N., Duflo H., Tinel A.** and **Duclos J.** Lamb wave reflection at the free edge of a plate. Journal of the Acoustical Society of America. 2003. Vol. 113**. Issue 3. P. 1417–1425.

26. **Kaplunov J. D.** et al. Free localized vibrations of a semi-infinite cylindrical shell. Journal of the Acoustical Society of America. 2000. Vol. 107, Issue 3. P. 1383-1393.

27. **Silk M. G., Bainton K. F.** The propagation in metal tubing of ultrasonic wave modes equivalent to Lamb waves, Ultrasonics. 1979. Vol. 17. P. 11–

28. **Gazis D. C.**. Three-dimensional investigation of the propagation of waves in hollow circular cylinders. I. Analytical foundation, Journal of the Acoustical Society of America. 1959. Vol. 31. Issue 5. P. 568-573.

29. **Meitzler A. H.**. Mode Coupling in the Propagation of Elastic Pulses in Wires Journal of the Acoustical Society of America. 1961. Vol. 33. Issue 4. P. 435-445.

Appendix A

For detailed analysis, reader is referred to look into following publication [29]. Demanding stress free surfaces of the tube at $r = a$ and $r = b$ in case $n = 0$ (Fig.1) leads to the dispersion frequency equation for axisymmetric longitudinal modes

$$G \cdot C = \begin{bmatrix} G_{11} & G_{12} & G_{13} & G_{14} \\ G_{21} & G_{22} & G_{23} & G_{24} \\ G_{31} & G_{32} & G_{33} & G_{34} \\ G_{41} & G_{42} & G_{43} & G_{44} \end{bmatrix} \begin{bmatrix} C_1 \\ C_2 \\ C_3 \\ C_4 \end{bmatrix} = 0, \quad \text{(A.1)}$$

where

$$G_{11} = -(\beta^2 - \xi^2)a^2 J_0(\alpha a) + 2\alpha a J_1(\alpha a),$$

$$G_{12} = 2\xi\beta a^2 J_0(\beta a) - 2\xi a J_1(\beta a),$$

$$G_{13} = -(\beta^2 - \xi^2)a^2 N_0(\alpha a) + 2\alpha a N_1(\alpha a),$$

$$G_{14} = 2\xi\beta a^2 N_0(\beta a) - 2\xi a N_1(\beta a),$$

$$G_{21} = 2\xi\alpha a^2 J_1(\alpha a),$$

$$G_{22} = (\beta^2 - \xi^2)a^2 J_1(\beta a),$$

$$G_{23} = 2\xi\alpha a^2 N_1(\alpha a),$$

$$G_{24} = (\beta^2 - \xi^2)a^2 N_1(\beta a).$$

$$\text{(A.2)}$$

Here

$$\alpha^2 = \omega^2 / c_L^2 - \xi^2, \quad \beta^2 = \omega^2 / c_T^2 - \xi^2, \quad \text{(A.3)}$$

c_L and c_T – velocities of compressional and shear waves of the medium, $\omega = 2\pi f$ – ring frequency, ξ – axial wave number, J, N – Bessel functions. The remaining two rows of the system (A.1) are obtained from the first two by substitution of b for a. To obtain nontrivial eigen solutions ξ, the characteristic equation should be

$$Det[G] = 0. \quad \text{(A.4)}$$

Using notations

$$f(r) = C_1 J_0(\alpha r) + C_3 N_0(\alpha r), \quad \text{(A.5)}$$

$$h(r) = C_2 J_1(\beta r) + C_4 N_1(\beta r), \quad \text{(A.6)}$$

the displacements and stresses are

$$u_r = (\partial f / \partial r + \xi h)e^{i(\xi z - \omega t)},$$
$$u_z = i(\xi f + h / r + \partial h / \partial r)e^{i(\xi z - \omega t)}, \quad \text{(A.7)}$$

$$\sigma_{rr} = \left[-\lambda(\alpha^2 + \xi^2)f + 2\mu\left(\partial^2 f / \partial r^2 + \xi\partial h / \partial r\right)\right]e^{i(\xi z - \omega t)},$$
$$\sigma_{rz} = i\mu\left[2\xi\partial f / \partial r + \left(\xi^2 - \beta^2\right)h\right]e^{i(\xi z - \omega t)},$$
$$\sigma_{zz} = \left[-\lambda(\alpha^2 + \xi^2)f - 2\mu\xi(\xi f + h / r + \partial h / \partial r)\right]e^{i(\xi z - \omega t)},$$

$$\text{(A.8)}$$

where λ and μ are Lamé's constants.